

Generation of Fourier-transform-limited heralded single photons

Alfred B. U'Ren,¹ Yasser Jeronimo-Moreno,¹ and Hipolito Garcia-Gracia²

¹*División de Física Aplicada, Centro de Investigación Científica y Educación Superior de Ensenada (CICESE), Baja California, 22860, Mexico*

²*Photonics and Mathematical Optics Group, Tecnológico de Monterrey, Nuevo León, 64849, Mexico*
(Received 22 June 2006; revised manuscript received 10 November 2006; published 15 February 2007)

In this paper we study the spectral (temporal) properties of heralded single photon wave packets, triggered by the detection of an idler photon in the process of parametric down conversion. The generated single photons are studied within the framework of the chronocyclic Wigner function, from which the single photon spectral width and temporal duration can be computed. We derive specific conditions on the two-photon joint spectral amplitude which result in both pure and Fourier-transform-limited heralded single photons. Likewise, we present specific source geometries which lead to the fulfillment of these conditions and show that one of these geometries leads, for a given pump bandwidth, to the temporally shortest possible heralded single photon wave packets.

DOI: [10.1103/PhysRevA.75.023810](https://doi.org/10.1103/PhysRevA.75.023810)

PACS number(s): 42.50.Ar, 03.67.–a

I. INTRODUCTION

Single photon wave packets are a crucial ingredient for a number of quantum-enhanced technologies such as quantum computation with linear optics [1] and secure quantum key distribution [2]. Recently it has been shown that single photons can be efficiently “heralded,” whereby photon pairs are generated by the process of spontaneous parametric down conversion (PDC) and subsequently one of the photons is detected, thus conditionally preparing a single photon wave packet in the conjugate mode [3–7]. While great progress has been made in the development of so-called on demand single photon sources (e.g., based on quantum dots in microcavities [8], single atoms coupled to optical cavities [9], and nitrogen vacancies in diamond [10]), PDC can lead to practical, room-temperature sources of heralded single photons. A crucial property of PDC-based heralded single photon sources is that the spatial and spectral emission properties can be controlled to a large degree by appropriate choices of the source geometry, including dispersion characteristics of the nonlinear crystal, and the pump characteristics. It is indeed remarkable that PDC can be configured to produce photon pairs ranging from those which are factorable to those which are highly entangled in continuous degrees of freedom such as frequency and transverse wave vector. In this paper, we exploit this flexibility to derive conditions for the generation of both pure *and* Fourier-transform-limited heralded single photons. Likewise, we present specific source geometries which lead to the fulfillment of such conditions. Thus, the techniques presented here can be used to design PDC photon pair sources leading to heralded single photons described by Fourier-transform (FT) limited, ultrashort wave packets.

Heralded single photon sources rely on the quality of the photon-number correlations between the signal and idler (used as trigger) PDC modes. It is experimentally straightforward to determine such quality by measuring the ratio of the coincidence detection rate across the signal and trigger PDC modes to the signal singles count rate. There are a number of experimental factors which can reduce this ratio from its ideal unity value. Higher-order PDC contributions

whereby more than one photon pair can be emitted at a given time implies that a trigger detection event (from a nonphoton number resolving detector) can erroneously indicate the presence of a single signal photon, while in reality two, or more, photons are present. Likewise, the presence of optical losses in the signal mode implies that a trigger detection event can erroneously indicate the presence of a single signal photon, while in reality a vacuum state exists. The presence of background photons, for which a trigger is detected without the existence of a signal photon evidently also reduces the heralding efficiency. In Ref. [4] we have proposed and implemented an experimental criterion which assesses source performance, specifically suited to heralded single photon sources, including the effects of optical losses, higher photon number contributions, background photons, and the binary behavior of realistic single photon detectors.

Apart from the quality of photon number correlations between the two PDC modes, it is important to consider how entanglement in continuous degrees of freedom (e.g., spectral and transverse wave vector) translates into the properties of the heralded single photon. Specifically, as was shown in Ref. [13], correlations in any degree of freedom in the photon pairs results in a departure from purity in the heralded single photons. Such impurity is undesirable because it implies that multiple single photons produced by more than one source will not interfere. In this paper we further analyze the spectral (temporal) properties of heralded single photon wave packets, showing for a restricted class of states that factorable photon pairs lead to both *pure* and *Fourier-transform-limited* heralded single photons. We show in addition that in a specific source geometry the heralded single photons can attain their shortest possible temporal duration, which corresponds to the pump pulse duration.

II. DESCRIPTION OF HERALDED SINGLE PHOTONS

The heralded single photon in the signal mode can be represented by its density operator $\hat{\rho}_s$

$$\hat{\rho}_s = \text{Tr}_i(\hat{\rho}\hat{\Pi}_i), \quad (1)$$

where Tr_i represents a partial trace over the trigger mode, in terms of the density operator of the two photon state $\hat{\rho}$ and of

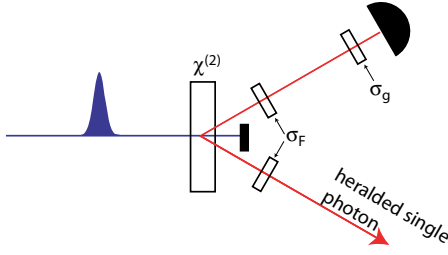


FIG. 1. (Color online) Heralded single photon source, based on pulsed parametric down conversion in a $\chi^{(2)}$ crystal.

the measurement operator $\hat{\Pi}_t$ for the trigger (idler) mode

$$\hat{\Pi}_t = \int d\omega g(\omega) |\omega\rangle_i \langle \omega|_i, \quad (2)$$

which has been expressed in terms of the frequency-dependent trigger detection efficiency $g(\omega)$.

We will consider a heralded single photon source based on the process of parametric down conversion (PDC) pumped by an ultrashort pulse, shown schematically in Fig. 1. The two-photon state for the PDC process assuming specific directions of propagation (i.e., disregarding the transverse wave vector degree of freedom) can be expressed as

$$|\Psi\rangle = \int \int d\omega_s d\omega_i f(\omega_s, \omega_i) |\omega_s\rangle_s |\omega_i\rangle_i, \quad (3)$$

where $|\omega_\mu\rangle = \hat{a}^\dagger(\omega_\mu) |\text{vac}\rangle_\mu$ with $\mu = s, i$ in terms of the joint spectral amplitude (JSA)

$$f(\omega_s, \omega_i) = \Phi(\omega_s, \omega_i) \alpha(\omega_s + \omega_i) F(\omega_s, \omega_i), \quad (4)$$

which is in turn given by the product of the phase matching function (PMF) $\Phi(\omega_s, \omega_i)$, the pump envelope function (PEF) $\alpha(\omega_s + \omega_i)$ and a filter function $F(\omega_s, \omega_i)$. While the PMF contains information about the optical properties of the nonlinear crystal, the PEF characterizes the pump field utilized. The function $F(\omega_s, \omega_i)$ describes the action of identical spectral filters (labeled σ_F in the figure) acting on both generated photons. The JSA is assumed to be normalized so that the integral over both frequency arguments of its absolute value squared yields unity. Substituting the two-photon density operator $\hat{\rho} = |\Psi\rangle\langle\Psi|$ into Eq. (1), we arrive at the following expression for the density operator which results for the heralded single photon in the signal mode

$$\hat{\rho}_s = \int_0^\infty d\omega_0 g(\omega_0) |\phi(\omega_0)\rangle \langle \phi(\omega_0)|, \quad (5)$$

where

$$|\phi(\omega_0)\rangle = \int_0^\infty d\omega_1 f(\omega_1, \omega_0) |\omega_1\rangle_s. \quad (6)$$

Let us note that, in contrast to the two-photon density operator $\hat{\rho} = |\Psi\rangle\langle\Psi|$, in general the single photon density operator $\hat{\rho}_s$ represents a mixed state. In order to gain physical insight, let us consider the case where spectral filtering is

applied to the trigger mode (such a filter is labeled σ_g in Fig. 1). In the limit of strong filtering we may write the trigger detection efficiency as a delta function $g(\omega) \rightarrow \delta(\omega - \omega_F)$. Under these circumstances, the resulting single photon density operator is given by

$$\hat{\rho}_s = |\phi(\omega_F)\rangle \langle \phi(\omega_F)|, \quad (7)$$

which evidently represents a pure state [11]. Thus, an avenue towards a pure heralded single photon source is to implement strong spectral filtering on the trigger mode. However, this is achieved at the cost of a reduction in source brightness as well as a reduction in the bandwidth of the prepared photon through nonlocal state projection.

Is it possible to obtain a pure state without resorting to strong spectral filtering? Let us consider the case where the joint spectral amplitude $f(\omega_s, \omega_i)$ is factorable, i.e., where functions $p(\omega)$ and $q(\omega)$ exist such that $f(\omega_s, \omega_i) = p(\omega_s)q(\omega_i)$. It is straightforward to show from Eqs. (5) and (6) that under these circumstances the heralded single photon is indeed pure. In order to gain understanding of the conditions for single photon purity, let us perform a Schmidt decomposition of the two photon state. The JSA can now be expressed as

$$f(\omega_s, \omega_i) = \sum_m \sqrt{\lambda_m} u_m(\omega_s) v_m(\omega_i), \quad (8)$$

where $u_m(\omega)$ and $v_m(\omega)$ represent the Schmidt functions and λ_m represents the Schmidt eigenvalues [12]. The resulting two photon density operator $\hat{\rho}_s$ can be expressed as

$$\hat{\rho}_s = \sum_m \sum_n \sqrt{\lambda_m \lambda_n} \int d\omega_0 g(\omega_0) v_m(\omega_0) v_n^*(\omega_0) |\phi_m\rangle \langle \phi_n|, \quad (9)$$

in terms of the Schmidt single photon wave packets

$$|\phi_m\rangle = \int d\omega u_m(\omega) |\omega\rangle_s. \quad (10)$$

It is evident from Eq. (9) that in general the heralded single photon is described by a mixed state, given as an incoherent sum of the Schmidt wave packets. This expression simplifies considerably in the case where the trigger detection efficiency is not frequency dependent; using orthogonality of the Schmidt functions, Eq. (9) then reduces to

$$\hat{\rho}_s = \sum_m \lambda_m |\phi_m\rangle \langle \phi_m|. \quad (11)$$

From an analysis of Eqs. (9) and (11) it becomes clear that if the two photon state contains a single pair of Schmidt modes, i.e., if there is a single term in the sum in Eq. (8), the resulting heralded single photon state is pure. Thus, by engineering the state *at the source* so as to guarantee factorability (for which the state is expressed in terms of a single Schmidt mode pair), it becomes possible to achieve pure single photon conditional generation without resorting to spectral filtering. Conversely, for a progressively larger number of active Schmidt mode pairs in the photon pair, the attainable single photon purity decreases. Indeed, as was shown in Ref. [13],

the single photon purity $p = \text{Tr}(\hat{\rho}_s^2)$ is given by $p = 1/K$ where the Schmidt number K is a measure of the number of active mode pairs. In this case, a pure heralded single photon may still be obtained by spectral filtering at the cost of a reduction in both single photon bandwidth *and* signal level. Thus factorable photon pair generation represents a crucial enabling technology for future progress in experimental quantum information processing.

III. CHRONOCYCLIC WIGNER FUNCTION

It is convenient to study the temporal and spectral properties of heralded single photons within the framework of the chronocyclic Wigner function (CWF) formalism. The latter represents a useful tool for the description of classical ultrashort pulses [14,15] and it has also been used to represent the PDC two-photon state [16]. In this paper, we consider the CWF for the heralded single photon, which can be expressed in terms of the single photon density operator $\hat{\rho}_s$ as

$$W_s(\omega, t) = \frac{1}{2\pi} \int_{-\infty}^{\infty} d\omega' \langle \omega + \omega'/2 | \hat{\rho}_s | \omega - \omega'/2 \rangle e^{i\omega' t}, \quad (12)$$

where subscripts s in the frequency bra and ket have been omitted for clarity. Such a function fully characterizes the spectral and temporal properties of the single photons; indeed, the marginal distribution resulting from integrating the CWF over frequency or time results in the temporal or spectral, respectively, single photon intensity profile. In terms of the joint spectral amplitude $f(\omega_s, \omega_i)$, the chronocyclic Wigner function for the heralded single photon can be expressed as

$$W_s(\omega, t) = \frac{1}{2\pi} \int d\omega_0 g(\omega_0) \int d\omega' f\left(\omega + \frac{\omega'}{2}, \omega_0\right) \times f^*\left(\omega - \frac{\omega'}{2}, \omega_0\right) e^{i\omega' t}. \quad (13)$$

Let us note that the chronocyclic Wigner function, as expressed in Eq. (13), is a generalization of the Wigner-Ville function [14] for a spectral amplitude function $f(\omega_1, \omega_2)$ which depends on two rather than one variable; the additional integration over the second frequency argument results from tracing over one of the two photons in the heralding process.

The spectral intensity profile of the heralded single photons is given by the integral over the time variable of the chronocyclic Wigner function

$$I_\omega(\omega) = \int dt W_s(\omega, t) = \int d\omega_0 g(\omega_0) |f(\omega, \omega_0)|^2, \quad (14)$$

while the temporal intensity profile is given by the integral over the frequency variable of the chronocyclic Wigner function

$$I_t(t) = \int d\omega W_s(\omega, t) = \frac{1}{2\pi} \int d\omega_0 g(\omega_0) \left| \int d\omega f(\omega, \omega_0) e^{i\omega t} \right|^2. \quad (15)$$

In terms of the Schmidt functions, we may express the CWF as

$$W_s(\omega, t) = \frac{1}{2\pi} \sum_n \sum_m \sqrt{\lambda_m \lambda_n} \int d\omega_0 g(\omega_0) v_m(\omega_0) v_n^*(\omega_0) \times \int d\omega' u_m\left(\omega + \frac{\omega'}{2}\right) u_n^*\left(\omega - \frac{\omega'}{2}\right) e^{i\omega' t}. \quad (16)$$

If the trigger detection efficiency is not frequency dependent, using orthogonality of the Schmidt functions, Eq. (16) reduces to

$$W_s(\omega, t) = \frac{1}{2\pi} \sum_m \lambda_m \int d\omega' u_m\left(\omega + \frac{\omega'}{2}\right) u_m^*\left(\omega - \frac{\omega'}{2}\right) e^{i\omega' t}. \quad (17)$$

In this case, the spectral and temporal intensity profiles are given by

$$I_\omega(\omega) = \sum_m \lambda_m |u_m(\omega)|^2, \quad (18)$$

$$I_t(t) = 2\pi \sum_m \lambda_m |\tilde{u}_m(t)|^2, \quad (19)$$

where $\tilde{u}_m(t)$ represents the Fourier transform of $u_m(\omega)$. In order to carry out more explicit calculations, we will assume PDC photon pairs within a restricted, though quite general, class of states. We will consider a frequency-degenerate collinear PDC source (centered at frequency ω_c) based on type-II phase matching, pumped by a short pulse (centered at frequency $2\omega_c$) and will disregard group velocity dispersion (as well as higher-order dispersion) terms. The phase matching function for such an interaction can be expressed as follows

$$\phi(\omega_s, \omega_i) = \text{sinc}[L\Delta k(\omega_s, \omega_i)/2] \exp[iL\Delta k(\omega_s, \omega_i)/2], \quad (20)$$

with the phase mismatch expressed as a Taylor series up to first order

$$L\Delta k(\omega_s, \omega_i) \approx L\Delta k^{(0)} + \tau_s(\omega_s - \omega_c) + \tau_i(\omega_i - \omega_c), \quad (21)$$

in terms of the PDC central frequency ω_c , the constant term of the Taylor series $\Delta k^{(0)}$ (which we assume to vanish) and the longitudinal temporal walkoff terms between the pump pulse and each of the signal and trigger photons

$$\tau_s = L[k'_p(2\omega_c) - k'_s(\omega_c)], \quad (22)$$

$$\tau_i = L[k'_p(2\omega_c) - k'_i(\omega_c)]. \quad (23)$$

Let us note that by retaining only constant and group velocity terms, we ignore temporal broadening effects resulting from quadratic and higher order dispersion terms. While evi-

dently a complete analysis should include these terms, for the case analyzed in detail here which corresponds to collinear, degenerate type-II PDC where the bandwidth of the generated light is somewhat restricted (as compared, for example, to collinear, degenerate type-I PDC), the group velocity approximation is justified. We model the pump envelope function as a Gaussian function with width σ

$$\alpha(\omega_s + \omega_i) = \exp\left[-\frac{(\omega_s + \omega_i - 2\omega_c)^2}{\sigma^2}\right]. \quad (24)$$

In order to obtain an analytic expression for the CWF in closed form, we approximate the sinc function appearing in the phase matching function [see Eq. (20)] as a Gaussian function [$\text{sinc}(x) \approx \exp(-\gamma x^2)$ with $\gamma \approx 0.193$]. As we will discuss below, comparisons of the CWF calculated numerically without resorting to approximations and the analytic CWF suggest that the Gaussian approximation represents a valid approximation in that it yields a useful indication of the single photon bandwidth and temporal duration. Likewise, we assume a Gaussian shape (with central frequency ω_{g0} and bandwidth σ_g) for the trigger detection efficiency $g(\omega)$ [see Eq. (5)]

$$g(\omega) = \exp\left[-\frac{(\omega - \omega_{g0})^2}{\sigma_g^2}\right], \quad (25)$$

and a Gaussian shape for the two-photon filter function $F(\omega_s, \omega_i)$ with width σ_F

$$F(\omega_s, \omega_i) = \exp\left[-\frac{(\omega_s - \omega_c)^2 + (\omega_i - \omega_c)^2}{\sigma_F^2}\right]. \quad (26)$$

Carrying out the integrals we obtain a CWF of the following form

$$W_s(\omega, t) = \frac{1}{\pi\Delta\omega\Delta t} \exp\left(-\frac{[\omega - \omega_c + \Omega]^2}{\Delta\omega^2}\right) \times \exp\left(-\frac{[t - T]^2}{\Delta t^2}\right), \quad (27)$$

in terms of the temporal and spectral widths Δt and $\Delta\omega$,

$$\Delta t = T_{ss}, \quad (28)$$

$$\Delta\omega = \frac{T_{ii}}{\sqrt{T_{ss}^2 T_{ii}^2 - T_{si}^4}}, \quad (29)$$

temporal and spectral shift terms T and Ω

$$T = \tau_s/2, \quad (30)$$

$$\Omega = \frac{1}{\sigma_g^2 T_{ss}^2 T_{ii}^2 - T_{si}^4} (\omega_{g0} - \omega_c), \quad (31)$$

where we have defined the quantities T_{ss} , T_{ii} , and T_{si} as follows

$$T_{ss}^2 = 2/\sigma_F^2 + 2/\sigma^2 + \gamma\tau_s^2/2, \quad (32)$$

$$T_{ii}^2 = 1/\sigma_g^2 + 2/\sigma_F^2 + 2/\sigma^2 + \gamma\tau_i^2/2, \quad (33)$$

$$T_{si}^2 = 2/\sigma^2 + \gamma\tau_s\tau_i/2. \quad (34)$$

It is straightforward to prove that for a two photon state for which its corresponding joint spectral amplitude can be expressed fully in terms of Gaussian functions, the spectral width $\Delta\omega$ and temporal duration Δt must satisfy the inequality $\Delta t\Delta\omega \geq 1$; here $\Delta\omega$ and Δt represent half widths at e^{-1} . Note that this is a particular instance of the uncertainty relation $\delta t\delta\omega \geq 1/2$ which is fulfilled for a broad class of functions (where δ refers to the standard deviation). However, the two photon state is given in terms of a sinc function, which does not have a well defined variance and therefore we cannot apply this result. Our approach is rather to use the Gaussian approximation in cases where it yields essentially the same chronocyclic Wigner function as without recourse to such an approximation, and employ the uncertainty relation associated with Gaussian functions. In order to study possible regimes resulting in Fourier-transform-limited conditional single photon generation, we compute the time-bandwidth (TB) product

$$\text{TB} = \Delta t\Delta\omega = (1 - T_{si}^4/T_{ss}^2 T_{ii}^2)^{-1/2}. \quad (35)$$

The quantity TB assumes its minimum value (TB=1) for Fourier transform limited single photons. Such photons are characterized by the important property that their temporal duration Δt is the shortest possible compatible with a given spectral width $\Delta\omega$. For single photons which are not Fourier transform limited, the time-bandwidth product assumes a value greater than unity; indeed, the specific value of TB provides a convenient measure of the departure from the Fourier transform limit. Clearly, the greater the numerical value of TB, the longer the time duration $\Delta t = \text{TB}/\Delta\omega$ for a given fixed spectral width.

Besides the temporal duration of the heralded single photon, another important characteristic time to consider is the correlation time: The time of emission *difference* between the signal and idler photons. Such a time is important because it defines the uncertainty in the expected detection time of the heralded photon relative to the detection of the trigger photon. In order to calculate the correlation time τ_c , we first compute the joint temporal intensity $|\tilde{f}(t_s, t_i)|^2$ where $\tilde{f}(t_s, t_i)$ denotes the two-dimensional Fourier transform of the joint spectral amplitude $f(\omega_s, \omega_i)$. The joint temporal intensity represents the probability density function for generating a photon pair at specific times t_s and t_i . As a second step, we may express the joint temporal intensity in terms of the variables $t_+ = t_s + t_i$ and $t_- = t_s - t_i$. From this, we can calculate the marginal probability distribution $S_-(t_-)$ which yields the probability density function for generating a photon pair with a certain time of emission difference t_- . For the approximations already introduced in this paper, we may express this t_- marginal distribution as $S_-(t_-) = \pi^{-1/2} \tau_c^{-1} \exp(-t_-^2/\tau_c^2)$ in terms of the correlation time τ_c

$$\tau_c = \frac{\sqrt{8 + \gamma\sigma_F^2(\tau_i - \tau_s)^2}}{\sqrt{2}\sigma_F}, \quad (36)$$

which in the absence of spectral filtering ($\sigma_F \rightarrow \infty$) reduces to

$$\tau_c = \sqrt{\gamma/2} |\tau_-|, \quad (37)$$

where

$$\tau_- = \tau_s - \tau_i = L[k'_s(\omega_c) - k'_i(\omega_c)]. \quad (38)$$

It is instructive to compare Eq. (28) [together with Eq. (32)] for the heralded single photon time duration with Eq. (37) [together with Eq. (38)] for the correlation time. It becomes apparent that while the former is defined by a group velocity mismatch term τ_s between the pump and the signal photon, the latter is defined by a group velocity mismatch term τ_- between the trigger and the signal photons. It should also be stressed that the correlation time *does not* depend on the pump bandwidth [17].

IV. FT-LIMITED SINGLE PHOTONS VIA GROUP VELOCITY MATCHING

In order to make the discussion more specific we will now consider the concepts developed so far for particular experimental situations. Let us first consider the case of PDC generation in the limit of vanishing pump bandwidth (i.e., $\sigma \rightarrow 0$). It is clear from Eqs. (28) and (32) that, when the pump bandwidth is much smaller than the reciprocal group velocity mismatch term (i.e., $\sigma \ll 1/\tau_s$), the single photon time duration becomes dependent only on the pump bandwidth: $\Delta t = \sqrt{2}/\sigma$. As might be expected this time duration tends to infinity in the idealized continuous wave (CW)-pump case. Likewise, the spectral width in the $\sigma \rightarrow 0$ limit can be computed from Eq. (29) and yields $\Delta\omega = \sqrt{2}/\gamma|\tau_-|$ (which in fact corresponds to the reciprocal (unfiltered) correlation time [see Eq. (37)]). Thus, the time bandwidth product in the limit of a very short pump bandwidth $TB = 2/(\sqrt{\gamma}\sigma|\tau_-|)$ diverges. We conclude therefore that CW-pumped PDC light is ill-suited for generation of Fourier-transform-limited heralded single photons.

Let us briefly consider degenerate, collinear type-I PDC as a candidate for ultrashort heralded single photon generation. Within the first order treatment presented in this paper [ignoring group velocity dispersion and higher order dispersive terms in the phase mismatch $\Delta k(\omega_s, \omega_i)$], degenerate collinear type-I photon pairs are characterized by $\tau_s = \tau_i$ or equivalently by $\tau_- = 0$. It has been shown [13] that the orientation of the phase matching function in $\{\omega_s, \omega_i\}$ space is given by $-\arctan(\tau_s/\tau_i)$, so that in the case of degenerate collinear type-I PDC, this orientation is fixed at -45° . Furthermore, within the linear approximation used, this function has an infinite extent along the direction $\omega_s - \omega_i$ and shows perfect overlap with the pump envelope function which is characterized by the same orientation: i.e., all frequency pairs within the pump envelope function are correctly phase matched. Thus, within this approximation the spectral width of each of the two single photon wave packets is infinite, while the temporal duration has a finite value, determined by the pump bandwidth and crystal length. Let us stress that the inclusion of GVD terms is necessary in the degenerate, collinear type-I case in order to obtain a physically meaningful

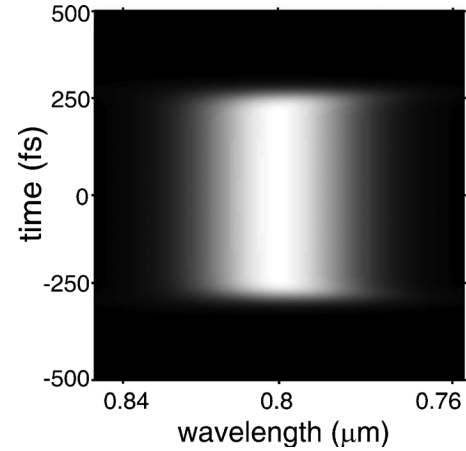


FIG. 2. Chronocyclic Wigner function (CWF) obtained numerically for a BBO crystal of 5 mm length, phase matched for collinear, degenerate type-I PDC centered at 800 nm, pumped by an ultrashort pulse train with a 5 nm bandwidth. The resulting single photon time duration $\Delta t = 288.01$ fs and single photon bandwidth $\Delta\omega = 61.4$ THz, with $\Delta t \Delta\omega \approx 17.7$, suggest a large departure from the transform limit.

result, leading to a very large (but finite) spectral bandwidth for each photon. The very large spectral bandwidth (which becomes extraordinarily large when the PDC photons are near the zero group velocity dispersion wavelength [19]), however, unfortunately does not result in ultrashort single photon wave packets [though it does imply a very short correlation time, see discussion above and Eqs. (36) and (37)]. In Fig. 2 we present the chronocyclic Wigner function [calculated numerically from Eq. (13)] for a specific collinear, degenerate type-I example. For a 5 mm long beta-barium-borate (BBO) crystal (with a cut angle of 29.2°), pumped by an ultrashort pulse train with 5 nm pump bandwidth producing photon pairs centered at 800 nm we obtain $\Delta t = 288.01$ fs and $\Delta\omega = 61.4$ THz, corresponding to $\Delta t \Delta\omega \approx 17.7$ [18] which suggests a large departure from the transform limit. Apart from the above considerations, let us note that degenerate, collinear type-I signal and idler photon pairs can at best be split probabilistically leading to a maximum heralding efficiency of 50%. Thus, we likewise conclude that degenerate, collinear type-I PDC is ill suited for generation of Fourier-transform-limited heralded single photons.

Let us turn our attention to the process of collinear, degenerate type-II PDC pumped by ultrashort pulses. In the propagation of short optical pulses through dispersive media, group velocity dispersion and higher dispersive terms result in temporal broadening, while group velocity terms result in propagation without distortion. The situation is somewhat different for the generation of PDC light by short pump pulses, where group velocity terms in the nonlinear crystal can result in photon pairs where the constituent single photon wave packets are temporally much longer than the pump pulse. We may write down the heralded single photon duration from Eq. (28) in terms of the pump pulse duration $\tau_p = \sqrt{2}/\sigma$ as

$$\Delta t = \tau_p \sqrt{1 + \frac{2}{\sigma_F^2 \tau_p^2} + \frac{\gamma \tau_s^2}{2 \tau_p^2}}. \quad (39)$$

It is evident from Eq. (39) that the shortest possible heralded single photon temporal duration is the pump pulse temporal duration itself. Likewise, we conclude from Eq. (39) that this shortest temporal duration is obtained in the limit of no spectral filtering ($\sigma_F \rightarrow \infty$) and of negligible group delay as compared to the pump pulse duration, i.e., $\tau_s \ll \tau_p$. It becomes apparent that for an ultrashort pump pulse, the attainable temporal duration is limited by the group velocity mismatch term τ_s . Two possibilities exist for making $\tau_s/\tau_p \ll 1$. The first involves using a very short crystal, concretely one obeying $L \ll \tau_p/(k'_p - k'_s)$; indeed for a short enough crystal the group delay τ_s due to group velocity mismatch can become insignificant. This involves the need for progressively shorter crystals as the pump pulse duration is decreased. It clearly does not represent a viable solution as it implies a prohibitive reduction in PDC flux. The second possibility is to employ a PDC interaction obeying group velocity matching between the pump and the PDC light. Indeed, it is clear from Eq. (39) that for $\tau_s=0$ (which implies $k'_p=k'_s$) we can obtain, with no spectral filtering, the shortest possible time duration τ_p irrespective of the crystal length used.

Let us stress that in our analysis in this paper, we have ignored group velocity dispersion terms (as well as higher order dispersive terms). For classical pulse propagation, under these circumstances we would expect no temporal broadening. However, Eq. (35) for the heralded single photon time-bandwidth product does indeed permit values greater than unity, even for an unchirped pump. The physical mechanism by which the single photon wave packets which constitute a PDC photon pair suffer temporal elongation is related to group velocity mismatch between the pump pulse and the generated PDC light. Indeed, in the long crystal limit the heralded single photon duration is determined purely by the group velocity mismatch term: $\Delta t_s \rightarrow \sqrt{\gamma} \tau_s / \sqrt{2}$. In order to understand this physically, let us consider a photon pair created on the second face of the crystal and secondly a photon pair created on the first face. While in the latter case the amplitudes for photon pair generation emerge from the crystal temporally overlapped with the pump pulse, in the former due to group velocity mismatch, these amplitudes emerge ahead of the pump pulse by a time τ_s . Because the wave packets corresponding to each of the two photons are the result of adding the amplitudes from all locations within the crystal, the result is a temporally stretched wave packet (as compared to the pump pulse). As a numerical example [to be discussed further below; see Fig. 3(c)], let us consider a 5 mm long BBO crystal pumped by a pulse train centered at 400 nm with 5 nm bandwidth. The expected duration of the wave packets computed from Eq. (28) is 127.2 fs (for a pump pulse with 28.3 fs duration), resulting in a time-bandwidth product of $TB=6.4$. As has already been discussed, for small pump bandwidths together with type-1 operation, the time bandwidth product can take much larger values; indeed it can be shown that values as high as 10^7 values of the Schmidt number K and TB are possible [19].

How can we achieve Fourier-transform-limited heralded single photon generation? An analysis of Eq. (35) reveals

that $TB=1$ if the correlation coefficient $T_{si}^2/(T_{ss}T_{ii})$ vanishes. One way in which this can occur is if strong filtering is applied to both photons ($\sigma_F \rightarrow 0$) or if strong filtering is applied to the trigger photon only ($\sigma_g \rightarrow 0$). In both of these cases, it can be readily shown that in the limit of strong filtering, the Fourier transform limit is attained (i.e., $TB \rightarrow 1$), evidently at the cost of a prohibitive reduction in flux. In addition, it should be stressed that while the FT limit may be attained via filtering, the bandwidth is thereby reduced thus precluding ultrashort single-photon wave packets. Alternatively, the correlation coefficient $T_{si}^2/(T_{ss}T_{ii})$ vanishes if $T_{si}=0$ which in fact represents the condition derived in Ref. [20] for spectral factorizability in photon pair states. Thus we reach the important conclusion that factorable two photon states [13,20,21,23] lead to Fourier-transform-limited heralded single photons. Let us note that the latter route involves no filtering, and therefore can lead to bright, broadband sources of FT-limited single photons.

An analysis of the CWF [see Eq. (12)] reveals that the single photon spectrum is in general shifted from the central PDC frequency ω_c by a frequency Ω [given by Eq. (31)] which depends linearly on the frequency detuning of the trigger filter with respect to the central PDC wavelength. Therefore, as the trigger filter passband is shifted, the resulting heralded single photon spectrum also shifts. This is a direct consequence of spectral correlation in the photon pair state; filtering of one of the two photons, nonlocally projects the conjugate photon into a particular spectral band. Indeed, Ω is proportional to T_{si} , which controls the degree of factorizability in the photon pair [20]. Thus, for a factorable two photon state (for which $T_{si}=0$) the heralded single photon spectrum does not shift due to shifts of the trigger filter passband. This suggests an experimental test for the degree of factorizability (and thus for the degree of departure from the FT limit).

The factorizability condition $T_{si}=0$ [see Eq. (34)] can be satisfied, for example, for the symmetric group velocity matching (SGVM) condition [20,22,23], expressed as $\tau_s + \tau_i = 0$, or alternatively as

$$2k'_p(2\omega_c) - k'_s(\omega_c) - k'_i(\omega_c) = 0. \quad (40)$$

Physically, this condition implies that the signal and idler photon amplitudes walk away longitudinally from the pump in a symmetric fashion: i.e., one outpaces the pump pulse by the same group delay as its conjugate lags the pump pulse. The resulting single photon temporal duration can be computed from Eq. (28) together with the conditions $\tau_s + \tau_i = 0$ and $T_{si}=0$ [see Eq. (34)], obtaining the result

$$\Delta t = \sqrt{2} \tau_p. \quad (41)$$

Thus, in the symmetric group velocity matching scenario, the single photon time duration assumes, within a factor of $\sqrt{2}$, its smallest possible value. It may be similarly shown that the spectral width is in this case simply the reciprocal of the temporal duration so that the Fourier transform limit is attained without recourse to filtering.

Let us study an alternative regime for Fourier transform limited single photon generation, where the pump group velocity is matched to the signal photon group velocity: i.e.,

$k'_p(2\omega_c) = k'_s(\omega_c)$ or $\tau_s = 0$, a regime which we refer to as asymmetric group velocity matching (AGVM). In this case, it may be readily shown that $TB \rightarrow 1$ if $\sigma\tau_i \gg 1$. The latter condition may be reexpressed as

$$\sigma L \gg \frac{1}{k'_p(2\omega_c) - k'_i(\omega_c)}. \quad (42)$$

Thus, by imposing the asymmetric group velocity matching condition together with a large crystal length-pump bandwidth product, it becomes possible to generate Fourier-transform-limited heralded single photons. AGVM is preferable over SGVM in the sense that for the former the heralded single photons attain the shortest possible time duration $\Delta t = \tau_p$ (equal to the pump duration) together with the largest FT-limited bandwidth possible $\Delta\omega = 1/\tau_p$ (while for the latter these parameters differ from the ideal values by a factor of $\sqrt{2}$). However, it should be stressed that AGVM leads to signal and idler photons which are distinguishable from each other; the former is not a limitation for heralded single photon generation but would be a limitation for experiments where the signal and idler photons are made to interfere with each other. Indeed, an advantage of the SGVM technique is that it combines ultrashort FT-limited heralded single photon generation with a symmetric joint spectral amplitude yielding indistinguishable signal and idler photons (except in polarization).

Another important aspect that should be considered when designing a heralded single photon source is the correlation time. This time determines the uncertainty in the expected time of arrival of the heralded single photon with respect to the trigger detection time. As has already been discussed, type-I PDC can result in extremely short correlation times, due to the larger PDC bandwidths possible. However, as has also been discussed, despite the short correlation times, type-I leads to states exhibiting a strong deviation from the FT limit. Let us compare heralded single photon sources resulting from SGVM and AGVM in terms of their correlation times. For SGVM, $\tau_s = -\tau_i$ and therefore Eq. (37) reduces to $\tau_c = \sqrt{2}\gamma|\tau_i|$, while for AGVM $\tau_s = 0$ and therefore Eq. (37) reduces to $\tau_c = \sqrt{\gamma/2}|\tau_i|$. When comparing these two results, it should be recalled that τ_i depends linearly on the crystal length and that in order to obtain a factorable state through AGVM, it is essential to use fairly long crystals [see Eq. (42)]. What this means in practice is that the correlation time tends to be much longer for heralded single photons produced through AGVM compared to heralded single photons produced through SGVM.

Let us consider specific examples to illustrate the single heralded photon duration and correlation time behavior. First, let us consider a 2 cm potassium dihydrogen phosphate (KDP) crystal cut at 67.7° (collinear, degenerate type-II emission at 830 nm) which can yield FT-limited single photons through AGVM [13]. Figure 3(a) shows the CWF computed numerically for this case, assuming a pump duration $\tau_p = 30.4$ fs (which corresponds to a 5 nm pump bandwidth). The resulting single photon duration under the Gaussian approximation is $\Delta t = \tau_p$ (where $\Delta\omega = 1/\Delta t$), while the correlation time is 896.3 fs. Secondly, let us consider a

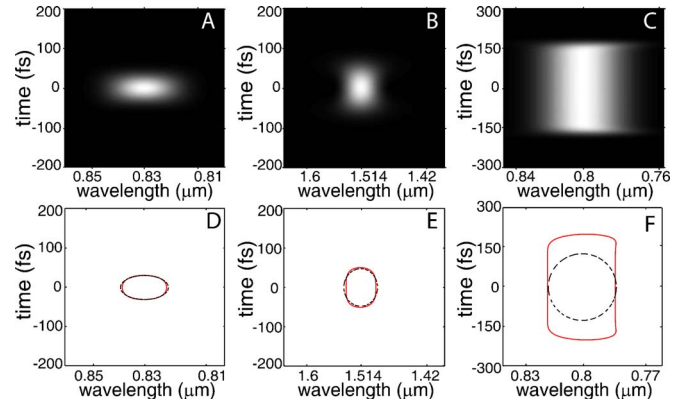


FIG. 3. (Color online) Panels (a)–(c) show examples of numerically calculated chronocyclic Wigner functions (CWF) without resorting to the Gaussian approximation and taking into account all dispersive orders, centered at a time $t=0$, for a single heralded single photon source based on (a) a KDP crystal, fulfilling asymmetric group velocity matching, (b) a BBO crystal, fulfilling symmetric group velocity matching, and (c) a BBO crystal not fulfilling any special group velocity condition. Panels (d)–(f) show, correspondingly to (a)–(c), the contour associated to one-half of the maximum value for the CWF calculated numerically (solid line) and for the CWF calculated analytically [dashed line; see Eq. (27)].

2.3-mm-length BBO crystal cut at 28.8° (collinear, degenerate type-II emission at 1514 nm) which can yield FT-limited single photons through SGVM [20]. Figure 3(b) shows the CWF computed numerically for this case, assuming a pump duration $\tau_p = 33.7$ fs (which corresponds to a 15 nm pump bandwidth). The resulting single photon duration under the Gaussian approximation is $\Delta t = \sqrt{2}\tau_p$ (where $\Delta\omega = 1/\Delta t$), while the correlation time is 67.5 fs (note this value is independent of the pump bandwidth used). Thus, while AGVM leads to the shortest possible time durations, it involves distinguishable signal and idler photons and longer correlation times as compared to SGVM.

In Fig. 3(c) we show, for comparison, the CWF corresponding to a PDC source which does not fulfill any particular group velocity condition and which therefore cannot be used as the basis for an FT-limited heralded single photon source. Here, we have assumed a 5-mm-length BBO crystal cut at 42.3° for collinear, degenerate type-II emission at 800 nm. The resulting single photon duration obtained numerically is $\Delta t = 205.7$ fs while the single photon bandwidth is $\Delta\omega = 50.1$ THz, yielding $\Delta t \Delta\omega \approx 10.3$ [18], which suggests a substantial deviation from the Fourier transform limit. Figures 3(d)–3(f) show the contour defined by frequencies and times for which the CWF takes a value of e^{-1} times the maximum value, calculated numerically (solid line) and analytically through Eq. (27) (dashed line) for each of the examples in Figs. 3(a)–3(c). In general terms, while the single photon bandwidth calculated numerically and analytically agree very well, the analytic result based on the Gaussian approximation tends to underestimate the temporal width. A computation of the temporal widths calculated numerically Δt_{nu} and analytically Δt_{an} while varying source parameters, such as crystal length and pump bandwidth (not shown) reveals that $\Delta t_{\text{nu}}/\Delta t_{\text{an}}$ ranges in value roughly from 1 to 1.6.

This is due to the difficulty of approximating top-hat-type functions (which result from a sinc-type structure in the spectral domain) with Gaussian functions. It should also be pointed out, however, that there is a class of PDC two-photon states for which the Gaussian approximation leads essentially to the same result as predicted without resorting to this approximation. This includes those states for which the crystal length L or the pump bandwidth σ (or both) are small. Furthermore, the maximum product $L\sigma$ for which the Gaussian approximation can be used reliably depends on the orientation of the PMF in signal-idler frequency space. Thus, for cases where the PMF is oriented vertically such as the AGVM example above, the sinc structure is fully contained by the idler single photon wave packet, which is traced over by heralding so that it has no effect on the prepared signal photon wave packet. The resulting agreement between the numerical and analytic calculations [see Fig. 3(d)] is essentially perfect; the very small disagreement is due to quadratic and higher order dispersion terms which are ignored by the analytic approach. Likewise, for the SGVM example above, the crystal is sufficiently short that the agreement is very good though the discrepancy is somewhat more apparent than for the AGVM example [see Fig. 3(e)]. Finally, for the third example shown, for which no particular GVM condition is fulfilled, the disagreement is more apparent. In this case while the analytic and numerical calculations both predict $\Delta\omega=50.1$ THz, the time durations obtained differ as follows: $\Delta t_{\text{an}}=127.2$ fs and $\Delta t_{\text{nu}}=205.7$ fs [see Fig. 3(f)].

We have shown that a factorable two-photon state leads to heralded single photons which are both pure and FT limited. We now address the question of what the relationship is, in general, between the Schmidt number K (which quantifies the departure from photon pair factorability) and the time-bandwidth product TB (which quantifies the departure for the single photons from the FT limit). Under the Gaussian approximation for the phase matching function it is possible to carry out an analytical Schmidt decomposition of the two photon state expressed in Eq. (3) [together with Eq. (4)]; such a calculation was carried out in Ref. [20]. For balanced filtering for both photons ($\sigma_g \rightarrow \infty$), it can be readily shown that the expression for the Schmidt number thus obtained is exactly identical to the expression we have derived for the time-bandwidth product TB [see Eq. (35)]. We therefore complement the results previously derived that the single photon purity p is the reciprocal of the Schmidt number [13] and in turn equal to the visibility V expected in a so-called event-ready Hong-Ou-Mandel (HOM) interferometer [24] (where two identical heralded single photons, from separate sources, are made to interfere in a HOM geometry) with the result that the time-bandwidth product is also equal to the Schmidt number. In summary, we arrive at the following equation linking the degree of spectral entanglement in the photon pairs (K) with important quantities relating to the resulting heralded single photon

$$K = \text{TB} = 1/p = 1/V. \quad (43)$$

While recent experiments demonstrate nearly ideal single photon heralding efficiencies, the generation of spectrally

pure, FT-limited single photon wave packets represents a challenge which must be addressed to make such sources useful for quantum information processing applications. In this context, the relationships expressed by Eq. (43) are important for the design of optimal heralded single photon sources. Equation (43) relates an important property of the photon pairs used (the degree of spectral entanglement, or Schmidt number K) with crucial properties of the resulting heralded single photons. These relationships suggest possible experimental procedures to determine source quality. Specifically, a measurement of the visibility in an event ready HOM interferometer would yield both the purity and the time-bandwidth product of the interfering single photon wave packets.

V. CONCLUSIONS

We have studied within the chronocyclic Wigner function (CWF) formalism the temporal (spectral) properties of heralded single photon sources based on the process of parametric down conversion, specifically in a type-II, collinear, frequency-degenerate regime. We have established, through a Gaussian approximation of the phase matching function, a clear relationship between the properties of the photon pairs generated by collinear, degenerate type-II PDC and those of the resulting heralded single photon. Despite the Gaussian approximation used, for an important subset of possible states, the CWF predicted analytically is essentially identical to that obtained numerically without recourse to approximations. We have shown that spectral entanglement in the photon pairs, as quantified by the Schmidt number, translates into spectral mixedness and a departure from the FT limit in the heralded single photons. Conversely, we have shown that factorable two photon states lead to both spectrally pure and Fourier-transform-limited heralded single photons. We have furthermore discussed two distinct group velocity matching scenarios both of which lead to factorable two photon states and therefore to pure and Fourier-transform-limited heralded single photons, without recourse to filtering. We have shown that heralded single photons obtained via asymmetric group velocity matching lead to the shortest possible single photon time duration, which corresponds to the pump pulse duration. The former is achieved, however, at the cost of a relatively large correlation time and of distinguishable signal and idler photons. Alternatively, heralded single photons based on symmetric group velocity matching lead to a single photon duration greater than the ideal value by a factor of $\sqrt{2}$ while exhibiting signal-idler indistinguishability and the lowest possible FT-limited correlation time. We believe these results may be important for the further development of practical single photon sources for quantum information processing.

ACKNOWLEDGMENTS

We acknowledge useful conversations with I. A. Walmsley, K. Banaszek, C. Silberhorn, and K. A. O'Donnell. This work was supported by Conacyt Grant No. 46370-F.

- [1] See, for example, review by P. Kok, W. J. Munro, K. Nemoto, T. C. Ralph, J. P. Dowling, and G. J. Milburn, e-print quant-ph/0512071.
- [2] See, for example, review by N. Gisin, G. G. Ribordy, W. Tittel, and H. Zbinden, *Rev. Mod. Phys.* **74**, 145 (2002).
- [3] A. B. U'Ren, C. Silberhorn, K. Banaszek, and I. A. Walmsley, *Phys. Rev. Lett.* **93**, 093601 (2004).
- [4] A. B. U'Ren, C. Silberhorn, J. L. Ball, K. Banaszek, and I. A. Walmsley, *Phys. Rev. A* **72**, 021802(R) (2005).
- [5] T. B. Pittman, B. C. Jacobs, and J. D. Franson, *Opt. Commun.* **246**, 545 (2005).
- [6] O. Alibart, D. B. Ostrowsky, P. Baldi, and S. Tanzilli, *Opt. Lett.* **30**, 1539 (2005).
- [7] S. Fasel, O. Alibart, S. Tanzilli, P. Baldi, A. Beveratos, N. Gisin, and H. Zbinden, *New J. Phys.* **6**, 163 (2004).
- [8] P. Michler, A. Kiraz, C. Becher, W. V. Schoenfeld, P. M. Petroff, Lidong Zhang, E. Hu, and A. Imamoglu, *Science* **290**, 2282 (2000); Z. Yuan, B. E. Kardynal, R. M. Stevenson, A. J. Shields, C. J. Lobo, K. Cooper, N. S. Beattie, D. A. Ritchie, and M. Pepper, *ibid.* **295**, 102 (2002); C. Santori, D. Fattal, J. V. Caronkovi, G. S. Solomon, and Y. Yamamoto, *Nature (London)* **419**, 594 (2002).
- [9] A. Kuhn, M. Hennrich, and G. Rempe, *Phys. Rev. Lett.* **89**, 067901 (2002).
- [10] C. Kurtsiefer, S. Mayer, P. Zarda, and H. Weinfurter, *Phys. Rev. Lett.* **85**, 290 (2000).
- [11] M. H. Rubin, *Phys. Rev. A* **61**, 022311 (2000).
- [12] C. K. Law, I. A. Walmsley, and J. H. Eberly, *Phys. Rev. Lett.* **84**, 5304 (2000).
- [13] A. B. U'Ren, Ch. Silberhorn, R. Erdmann, K. Banaszek, W. P. Grice, I. A. Walmsley, and M. G. Raymer, *Laser Phys.* **15**, 146 (2005).
- [14] J. Paye, *IEEE J. Quantum Electron.* **28**, 2262 (1992).
- [15] I. A. Walmsley and V. Wong, *J. Opt. Soc. Am. B* **13**, 2453 (1996).
- [16] W. P. Grice, Ph.D. thesis, University of Rochester, 1997 (unpublished).
- [17] S. Friberg, C. K. Hong, and L. Mandel, *Phys. Rev. Lett.* **54**, 2011 (1985).
- [18] In this case the CWF is not given by Gaussian functions, and therefore $\Delta t \Delta \omega \geq 1$ cannot be directly applied.
- [19] L. Zhang, A. B. U'Ren, R. Erdmann, K. A. O'Donnell, C. Silberhorn, K. Banaszek, and I. A. Walmsley, *J. Mod. Opt.* (to be published).
- [20] W. P. Grice, A. B. U'Ren, and I. A. Walmsley, *Phys. Rev. A* **64**, 063815 (2001).
- [21] V. Giovannetti, L. Maccone, J. H. Shapiro, and F. N. C. Wong, *Phys. Rev. Lett.* **88**, 183602 (2002); A. B. U'Ren, K. Banaszek, and I. A. Walmsley, *Quantum Inf. Comput.* **3**, 480 (2003); Z. D. Walton, A. V. Sergienko, B. E. A. Saleh, and M. C. Teich, *Phys. Rev. A* **70**, 052317 (2004); J. P. Torres, F. Macià, S. Carrasco, and L. Torner, *Opt. Lett.* **30**, 314 (2005); M. G. Raymer, J. Noh, K. Banaszek, and I. A. Walmsley, *Phys. Rev. A* **72**, 023825 (2005).
- [22] T. E. Keller and M. H. Rubin, *Phys. Rev. A* **56**, 1534 (1997).
- [23] O. Kuzucu, M. Fiorentino, M. A. Albota, F. N. C. Wong, and F. X. Kaertner, *Phys. Rev. Lett.* **94**, 083601 (2005).
- [24] A. B. U'Ren, Ph.D. thesis, University of Rochester, 2004.